

Journal of Biomedical Optics

BiomedicalOptics.SPIEDigitalLibrary.org

Transcranial low-level laser therapy enhances learning, memory, and neuroprogenitor cells after traumatic brain injury in mice

Weijun Xuan
Fatma Vatansever
Liyi Huang
Michael R. Hamblin

Transcranial low-level laser therapy enhances learning, memory, and neuroprogenitor cells after traumatic brain injury in mice

Weijun Xuan,^{a,b,c,†} Fatma Vatasever,^{b,c,†} Liyi Huang,^{b,c,d} and Michael R. Hamblin^{b,c,e,*}

^aRuikang Hospital Affiliated to Guangxi University of Chinese Medicine, Department of Otolaryngology, Nanning 530021, China

^bWellman Center for Photomedicine, Massachusetts General Hospital, Boston, Massachusetts 02114, United States

^cHarvard Medical School, Department of Dermatology, Boston, Massachusetts 02115, United States

^dGuangxi Medical University, First Affiliated College and Hospital, Department of Infectious Diseases, Nanning 530021, China

^eHarvard-MIT Division of Health Sciences and Technology, Cambridge, Massachusetts 02139, United States

Abstract. The use of transcranial low-level laser (light) therapy (tLLLT) to treat stroke and traumatic brain injury (TBI) is attracting increasing attention. We previously showed that LLLT using an 810-nm laser 4 h after controlled cortical impact (CCI)-TBI in mice could significantly improve the neurological severity score, decrease lesion volume, and reduce Fluoro-Jade staining for degenerating neurons. We obtained some evidence for neurogenesis in the region of the lesion. We now tested the hypothesis that tLLLT can improve performance on the Morris water maze (MWM, learning, and memory) and increase neurogenesis in the hippocampus and subventricular zone (SVZ) after CCI-TBI in mice. One and (to a greater extent) three daily laser treatments commencing 4-h post-TBI improved neurological performance as measured by wire grip and motion test especially at 3 and 4 weeks post-TBI. Improvements in visible and hidden platform latency and probe tests in MWM were seen at 4 weeks. Caspase-3 expression was lower in the lesion region at 4 days post-TBI. Double-stained BrdU-NeuN (neuroprogenitor cells) was increased in the dentate gyrus and SVZ. Increases in double-cortin (DCX) and TUJ-1 were also seen. Our study results suggest that tLLLT may improve TBI both by reducing cell death in the lesion and by stimulating neurogenesis. © 2014 Society of Photo-Optical Instrumentation Engineers (SPIE) [DOI: 10.1117/1.JBO.19.10.108003]

Keywords: traumatic brain injury; transcranial low level light therapy; Morris water maze; wire grip motion test; neurogenesis; BrdU; NeuN; double-cortin; TUJ-1; caspase-3; mitochondrial modulation.

Paper 140492R received Aug. 4, 2014; revised manuscript received Sep. 12, 2014; accepted for publication Sep. 15, 2014; published online Oct. 7, 2014.

1 Introduction

Severe traumatic brain injury (TBI) is a common cause of death and disability in industrialized countries.¹ In the US, each year 1.4 million people sustain TBIs, 235,000 patients are hospitalized and 50,000 die.² Furthermore, mild-TBI has recently attracted increasing attention due to its rising incidence after concussions in contact sports,³ and after blast injury in military conflicts.⁴ Although various anti-inflammatory and anti-apoptotic modalities have shown neuroprotective effects in experimental models of TBI, to date, no specific pharmacological agent aimed at blocking the progression of secondary brain damage has been approved for clinical use.⁵

For many years, adult brain morphogenesis and homeostasis was considered an exception (to the otherwise widely accepted developmental processes in an adult organisms and the role of stem cells therein) and the neural stem cells (NSCs) were thought to be present and effective only during brain developmental stages. The turning point in our perception was the discovery of adult neurogenesis and identification of cells that both *in vitro* and *in vivo* can function as NSCs generating neurons, glial cells, or both. The paradigm shift about the nature of the NSCs and potentials of the postnatal brain open the gates for new studies with a new outlook. Now, the scientific community

is engaged not only in depth understanding of the adult brain processes and NSCs functions, but also coupling them with novel treatment modalities.

Low-level laser (light) therapy (LLLT) using red or near-infrared (NIR) light appears to be one of these promising modalities. LLLT is gaining recognition as a viable treatment option for a diverse range of diseases and conditions characterized by injury, degeneration, inflammation, and pain.⁶ Transcranial LLLT (tLLLT) has already been proposed to treat traumatic and degenerative brain disorders⁷ and psychiatric disease.⁸ The mode of action is proposed to be that the photons produced by the light source are absorbed by components of the cellular mitochondrial respiratory chain increasing ATP and modulating reactive oxygen species and nitric oxide content, thus leading to activation of signaling pathways and transcription factors.⁹ Recently, we^{10–12} and others^{13–15} have shown that transcranially applied LLLT had significant beneficial effects in mouse models of severe TBI induced by either controlled cortical impact (CCI)^{10,13} or by closed head weight drop.^{11,14,15} We and others have shown that as a result of LLLT application, the neurological severity score is reduced,^{10–12,14,15} Morris water maze (MWM) performance improved¹³ and depression and anxiety levels were not only kept in check but also improved considerably.¹⁰ We also found that not only could tLLLT reduce the number of neurons undergoing degeneration (via Fluoro-Jade staining), suggesting

*Address all correspondence to: Michael R. Hamblin E-mail: hamblin@helix.mgh.harvard.edu

†These authors made an equal contribution to the paper.

neuroprotection, but that tLLLT could also increase bromodeoxyuridine (BrdU) positive cells in the vicinity of the brain lesion,¹² suggesting that the neurological improvement may be partly explained by the process of neurogenesis.¹⁶

Lately, adult neurogenesis has become a major topic of investigation in multiple classes of brain disease, including trauma^{17–18} degenerative diseases,¹⁹ and psychiatric disorders.²⁰ Many studies have suggested²¹ that the areas of the mammalian brain that are particularly specialized to produce proliferating neuroprogenitor cells are the subgranular layer of the dentate gyrus (DG) in the hippocampus,²² and the subventricular zone of the lateral ventricle.²³ The process of neurogenesis may be important in this acute TBI model where it can readily be seen after 4 weeks of follow-up that the neurological performance of the mice is improving; at the same time, the size of the cortical lesion is increasing.¹²

In this report, we describe improvements in learning and memory in mice with severe CCI-TBI treated either one or three times with daily tLLLT. Caspase-3 expression in the lesion was decreased at 4 days while BrdU-NeuN double stained cells together with DCX and TUJ-1 staining were increased at 7 days. The evidence for hippocampal and SVZ-neurogenesis suggests that newly formed neurons may play a role in repairing the brain lesion and regaining adequate brain function.

2 Materials and Methods

2.1 Animal Model

All animal procedures were approved by the Subcommittee on Research Animal Care (IACUC) of the Massachusetts General Hospital (Protocol No. 2010N000202) and met the guidelines of the National Institutes of Health. Young adult male BALB/c mice of 8 weeks (weight 21 to 25 g; Charles River Laboratories, Wilmington, MA) were used in the study. A detailed description of CCI-TBI induction, craniotomy procedure, and laser parameters is given in our previous publication.¹² Briefly, after the hairs on top of the head were removed with shaving and then depilated with Nair, the top of the skull was exposed with a skin incision of 1 cm (on central and sagittal direction). A careful 5-mm craniotomy was performed over the right parietotemporal cortex using a trephine attached to an electric portable drill without damaging the meninges. The bone flap was removed and the mouse brain was subjected to a controlled cortical impact using a special pneumatic impact device; pneumatic cortical impact device, Model AMS 201, AmScien Instruments LLC, Richmond, Virginia, with a 3-mm flat-tip, high pressure 150 psi, low pressure 30 psi, rod speed 4.8 m/s, rising duration 8.41 ms, and set impact depth of 2 mm that was adjusted to yield a moderate to severe TBI. One hour post-TBI induction, mice were given a neurological severity score (NSS) test and only those scoring 7–8 were included in the study (~75% of the injured mice). Immediately after generating the brain trauma, the craniotomy hole was sealed with bone wax and the skin was sutured. Mice were kept under anesthesia (with isoflurane) throughout the whole surgical procedure. Sham control mice were subjected to all aspects of the procedural steps except the actual cortical impact.

For this study, after severe CCI-TBI induction, mice were broadly divided into the following four groups: (a) sham TBI-sham laser treatment; (b) real TBI-sham laser treatment; (c) real TBI with one real laser treatment; (d) real TBI with three real laser treatments. The four broad groups (defined above) each

contained 16 mice per group with similar NSS values for the animals in groups b, c, and d to ensure comparable injury severity for all groups. Depending on the study group, mice were sacrificed at 4, 7, and 28 days post-TBI. Three mice per group were sacrificed on day 4 for caspase-3 determination. Five mice per group were sacrificed on day 7, and another five mice on day 28 for BrdU, DCX, and TUJ-1 immunofluorescence. The remaining three mice were sacrificed on day 29. This arrangement ensured that there were always (at least) eight mice alive per group to undergo performance and cognitive testing. The animals were housed as one mouse per cage and were maintained on a 12 h-light–12 h-dark cycle with access to food and water ad libitum.

2.2 Laser Treatment

Before laser irradiation (real or sham), mice were taped to a plastic plate via their paws. Sham TBI and real TBI mice received laser treatment (real or sham) once a day for either 1 day or for three consecutive days. Groups c and d received laser treatment with an 810-nm laser (DioDent Micro 810, HOYA ConBio, Fremont, California) delivering 18 J/cm² fluence and 25 mW/cm² irradiance for 12 min on a 1-cm spot diameter that covered the entire mouse head. Group c (with real TBI) received a single laser treatment 4 h post-TBI; group d (with real TBI) received one laser treatment per day for three consecutive days (the first irradiation being 4 h post-TBI).

2.3 Cognitive Performance Assessment

The MWM test was employed following a previously described protocol,²⁴ where the experimental set up for the MWM task consists of a circular swimming pool (110 cm diameter and 30 cm height) filled with water kept at 24°C. The target zone is the quadrant where the escape platform of 15 cm diameter was placed in a fixed position either visible or hidden (1 cm under the water surface). The other three quadrants were left, right, and opposite zones. Acquisition training consisted of trial blocks of two daily trials for 10 days, commencing at four different positions from the border of the maze in a semi-random order and with 15 min inter-trial intervals. If the platform was not found in 120 s, the mouse was placed on the platform for 15 s, and then returned to its cage. After the acquisition training, the actual trials started: the trial on the first day was latency to the visible platform; trials on the second day through sixth day

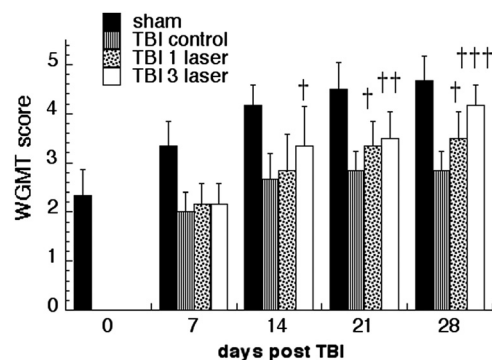


Fig. 1 The wire grip and motion test (WGMT) performed at four different time points; days 7, 14, 21, and 28 post-TBI induction. †, ††, ††† $P < 0.05, 0.01, 0.001$ versus traumatic brain injury (TBI).

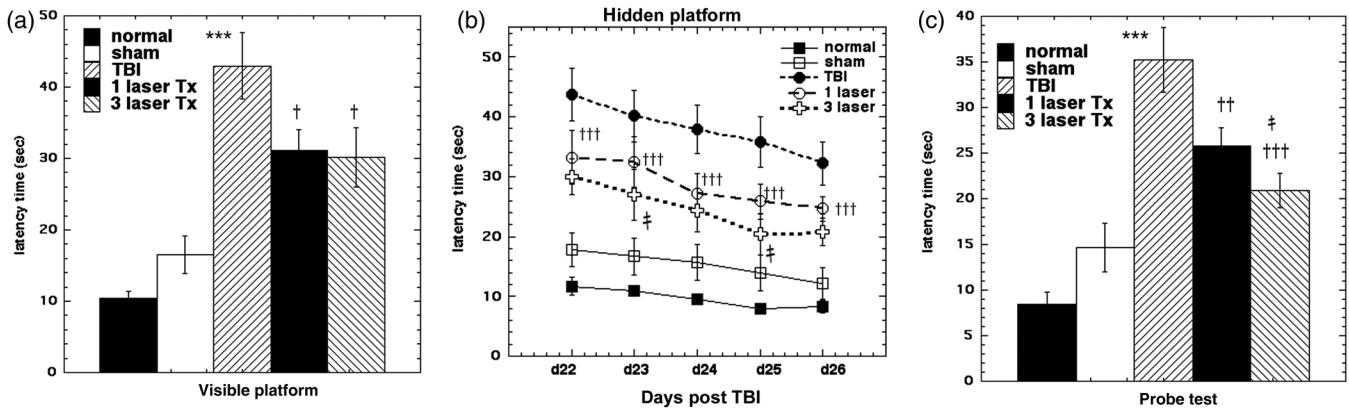


Fig. 2 Evaluating the effect of transcranial low-level laser (light) therapy (tLLLT) on cognitive performance of TBI sustained mice via Morris water maze test; (a) visible platform test, (b) hidden platform test, (c) probe test *** $p < 0.001$ versus sham; †, ††, ††† $P < 0.05, 0.01, 0.001$ versus TBI; ‡ $P < 0.05$ versus TBI 1 laser.

were latency to the hidden platform; the test at the seventh day was a probe trial where the platform was completely removed. MWM evaluations lasted from days 21–27 post-TBI.

2.4 Neuromotor Assessment

The wire grip and motion test (WGMT) was used to assess the motor function and muscle power via monitoring the grip strength and endurance where the mice were positioned on a horizontal wire of 0.6-mm thickness and 45-cm length, set at 46 cm above a tabletop. Assessment was done through grading the ability of the mouse to grip, retain position, and move along the wire. The test was performed in triplicate with an average value taken per mouse. WGMT was performed on days 0, 1, 4, 7, 10, 15, 19, 24, and 28.

2.5 Neurobehavioral Assessment

The neurological performance of the traumatized mice was routinely evaluated with the NSS test where mice were expected to perform 10 tasks measuring motor ability, balance, and alertness. The uninjured (control) mouse is given the score of zero and one point is added for each failed performance task, which can sum up to maximum score of 10. NSS evaluations started 1 h post-TBI (day 0) and were carried out on days 1, 4, 7, 10, 15, 19, 24, and 28. Mice with an NSS score less than 5 are assigned as sustained mild TBI; mice with an NSS score of 5–6 are assigned as sustained moderate TBI; an NSS score of 7–8 indicated mice sustaining severe TBI; an NSS score of 9–10 indicated mice sustaining very severe TBI. In our research, we studied mice sustaining severe TBI with an NSS of 7–8. The data showing the improvement of the NSS after tLLLT for

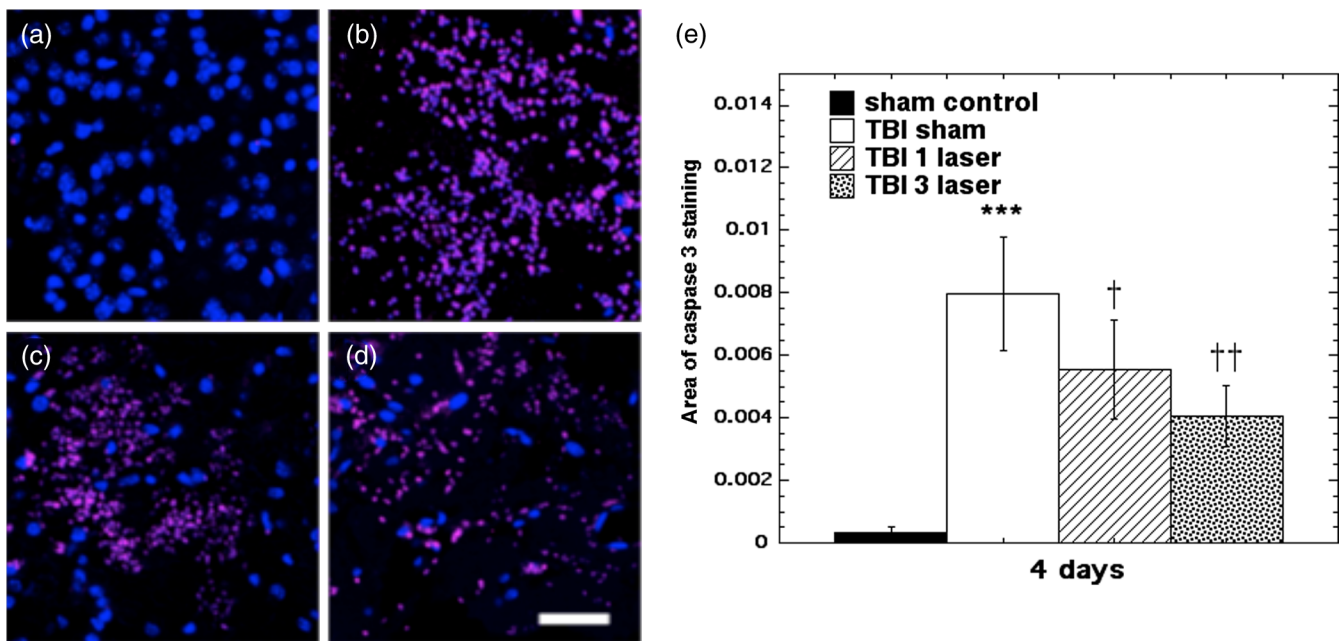


Fig. 3 Immunohistologic analysis for caspase-3 expression at the injury site, done at day 4 of the TBI induction. (a) sham, (b) CCI-TBI, (c) 1x tLLLT, (d) 3x tLLLT, (e) mean caspase-3/DAPI ratios \pm SD ($n = 5$). Scale bar 100 μm . *** $p < 0.001$ versus sham; †, †† $P < 0.05, 0.01$ versus TBI.

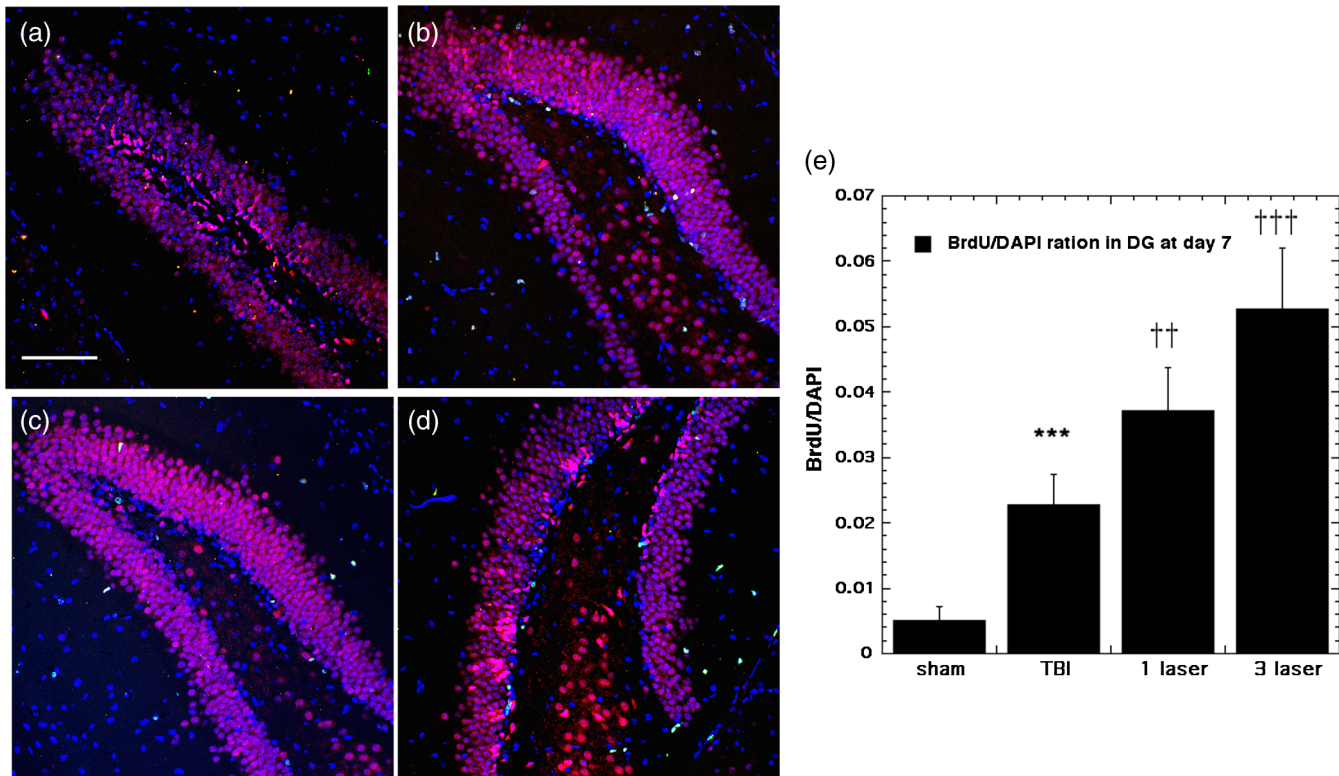


Fig. 4 BrdU-NeuN double-staining images and analyses at the neurogenic hippocampal DG at the 7 days point; (a) sham, (b) CCI-TBI, (c) 1× tLLLT, (d) 3× tLLLT, (e) mean BrdU/DAPI ratios \pm SD ($n = 5$); normalization of the readings was done BrdU versus DAPI (labeling the nuclei). Scale bar 100 μ m. *** $p < 0.001$ versus sham; ††, ††† $P < 0.01, 0.001$ versus TBI.

these TBI mice have already been reported, but it was necessary to repeat it for control of the injury severity.

2.6 Immunofluorescence Staining

Mice in the study groups were given a daily intraperitoneal injection of BrdU (Sigma, St. Louis, Missouri, Cat# B5002) as 50 mg/kg (diluted in saline) for seven consecutive days before sacrifice.

Mice (whose brains were to be studied) were anesthetized with isoflurane and perfused transcardially with 0.9% saline and then with 4% phosphate-buffered paraformaldehyde. Brains were excised and were fixed in the 4% phosphate-buffered paraformaldehyde solution for 3 days after which they were embedded in paraffin. Coronal serial brain cross sections of 5-mm thickness were taken and 10- μ -thick sections were cut from the top, middle, and bottom of the thick sliced blocks via microtome.

Immunofluorescence staining was performed using double staining for BrdU-NeuN, DCX, TUJ-1, and for caspase-3.

Brain sections to be double-stained for BrdU-NeuN underwent the standard immunofluorescence staining protocol for paraffin sections where (briefly) brain slices were mounted onto SuperFrostPlus charged glass slides followed by consecutive pretreatment with xylene for deparaffinization, graded ethanol for rehydration, and then passed through citrate buffer solution for antigen retrieval, followed with incubation with blocking solution of 5% BSA/0.1% Triton X-100 in phosphate-buffered saline. Immunostaining was done with a primary anti-body cocktail of rat anti-BrdU (Cat.# ab6326, abcam) and mouse anti-NeuN (Cat# MAB377, Millipore, Billerica, Massachusetts) for 72 h at 4°C to detect the neuronal cells. A cocktail of

secondary antibodies (Alexa fluor 488 conjugated anti-rat and Alexa fluor 568 conjugated anti-mouse, Invitrogen, Grand Island, New York) was used to stain the brain slices. Finally, they were cover slipped with mounting media containing DAPI (4',6-diamidino-2-phenylindole) (Cat#H-1200, Fisher Scientific, Waltham, Massachusetts). Cells positively stained for BrdU were imaged using a confocal microscope (Olympus America Inc., Center Valley, Pennsylvania) and then exported using Fiji software (Olympus Fluoview Version 3.0). For DCX staining we used rabbit anti-DCX (Cat# ab18723, Abcam, Cambridge, Massachusetts) and as a secondary the goat anti-rabbit Alexa fluor 568-conjugated (Invitrogen). For TuJ-1 staining we used mouse anti-TuJ-1 (Cat# MAB1637, Millipore) with the secondary anti-mouse Alexa fluor 488-conjugated (Invitrogen). Caspase-3 staining was done with rabbit anti-caspase-3 (Cat# 04-439, Millipore) and Alexa fluor 680-conjugated anti-rabbit as a secondary antibody (Invitrogen). Green BrdU, red DCX, or green TUJ-1 together with blue DAPI were quantified by the use of Image J (NIH, Bethesda, MD). Ratios of red or green fluorescence staining to blue DAPI fluorescence staining were calculated to normalize for the number of cells present in each microscopic field. Representative fields from five slides had the ratios averaged and the SD calculated.

2.7 Statistical Analyses

From each group in each brain area, we selected slices that showed more positive expression of each target antibody for comparison, and then respectively measured their positive expression area with Image-J software; finally, each target antibody expression area was divided by the DAPI area to normalize

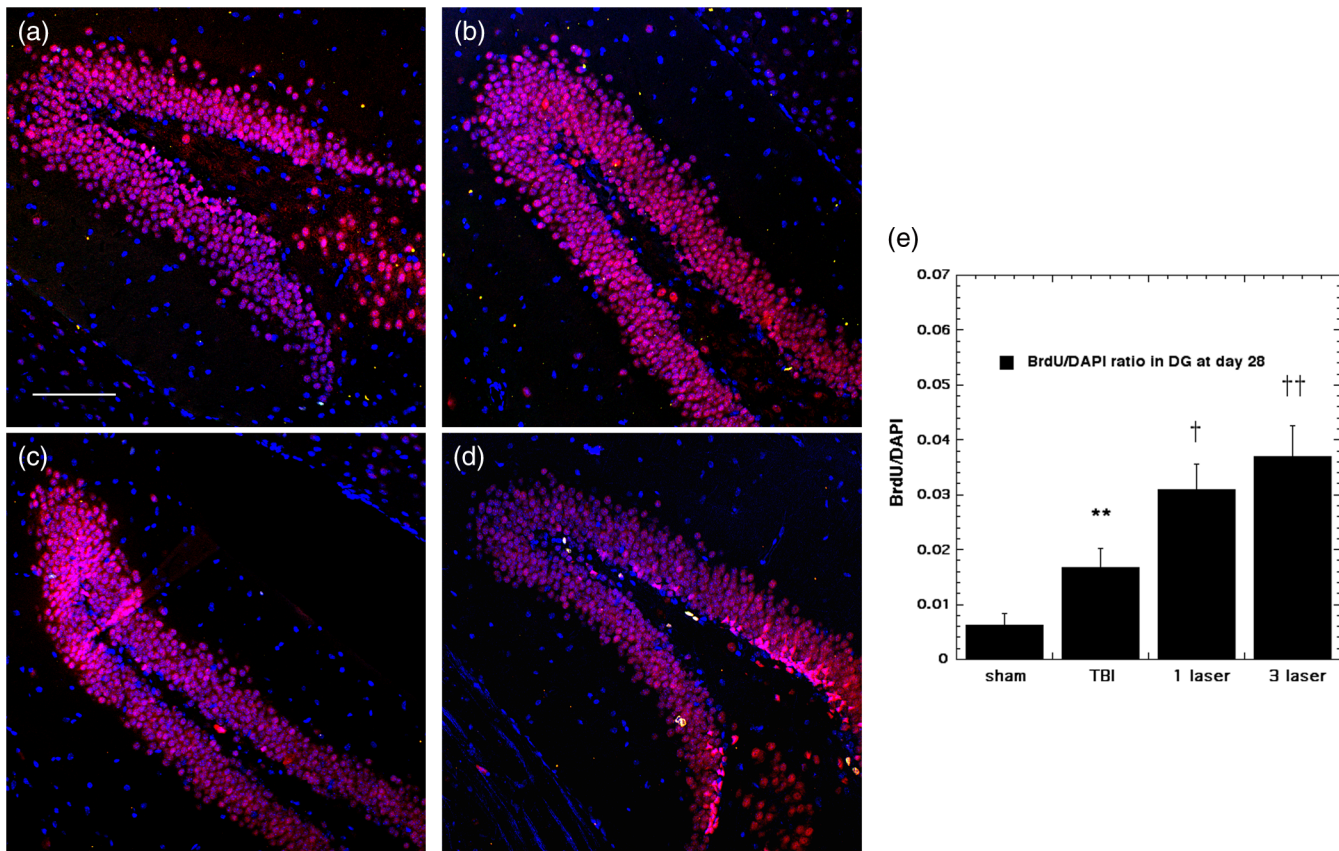


Fig. 5 BrdU-NeuN double-staining images and analyses at the neurogenic hippocampal DG at the 28 days point; (a) sham, (b) CCI-TBI, (c) 1× tLLLT, (d) 3× tLLLT, (e) mean BrdU/DAPI ratios \pm SD ($n = 5$); normalization of the readings was done BrdU versus DAPI (labeling the nuclei). Scale bar 100 μ m. ** $p < 0.01$ versus sham; †, †† $P < 0.05, 0.01$ versus TBI.

the data for the number of cells present. Data are presented as mean \pm SD, and analyzed using one-way analysis of variance followed by Tukey's post-hoc test. Significance was defined as $p < 0.05$. SPSS statistics V17.0 software was used for statistical analyses.

3 Results

3.1 Effect of Transcranial Low-Level Laser (Light) Therapy on Motor Function after Controlled Cortical Impact

We previously showed that the NSS score improved in CCI induction of TBI in mice treated with tLLLT.¹² Here, we also carried out the WGMT to show that another measure of neurological function improved in tLLLT treated mice. The WGMT performed at four different time points; days 7, 14, 21, and 28 post-TBI-induction, and the comparisons for the laser treatment effects are drawn against sham and TBI sustained cohorts. The overall improvement in the motor functions commences at day 14 of the CCI-TBI induction and at day 21 tLLLT applied cohorts show significant improvements: 1× tLLLT per day $p < 0.05$ and 3× tLLLT per day $p < 0.01$ against TBI sustained cohorts alone. At day 28, the improvements are even more pronounced: 3× tLLLT per day has $p < 0.001$ versus TBI, Fig. 1. Results are clearly indicate that the mice cohort that received three daily tLLLT exposures (3× tLLLT) showed a significant improvement ($p < 0.05$ versus TBI) in WGMT score at day

14 post-TBI. At day 21 post-TBI, both groups that received tLLLT (1× tLLLT $p < 0.05$ and 3× tLLLT $p < 0.01$) had significant improvements versus TBI and at day 28 the improvements were even more pronounced (1× tLLLT $p < 0.05$ and 3× tLLLT $p < 0.001$ versus TBI). Overall, 3× tLLLT proved to be more effective in improving the motor function.

3.2 Effect of Transcranial Low-Level Laser (Light) Therapy on Morris Water Maze Performance after Controlled Cortical Impact

The MWM study was carried out on days 21 through 27 post-TBI, Fig. 2. The groups were normal, sham-TBI, TBI, TBI 1× tLLLT, and TBI 3× tLLLT. The latency to the visible platform is shown in Fig. 2(a), the five daily repetitions of latency to the hidden platform are shown in Fig. 2(b), and the latency with the probe test is shown in Fig. 2(c). The visible platform latency is used to measure spatial navigation capabilities and the hidden platform test is used to measure the improvement in learning and memory, while the probe test is used to measure memory.

Our study shows that there was a large increase ($p < 0.001$) in latency to the visible platform in TBI mice (42 ± 4 s) compared to normal mice (10 ± 1 s) and sham-TBI mice (17 ± 3 s) as might be expected with brain damage. Both 1× tLLLT and 3× tLLLT produced significant improvements (31 ± 3 and 30 ± 4 s, respectively, compared to TBI mice ($p < 0.05$), Fig. 2(a).

With the five successive hidden platform trials, days 22 through 26, Fig. 2(b), there were again large increases

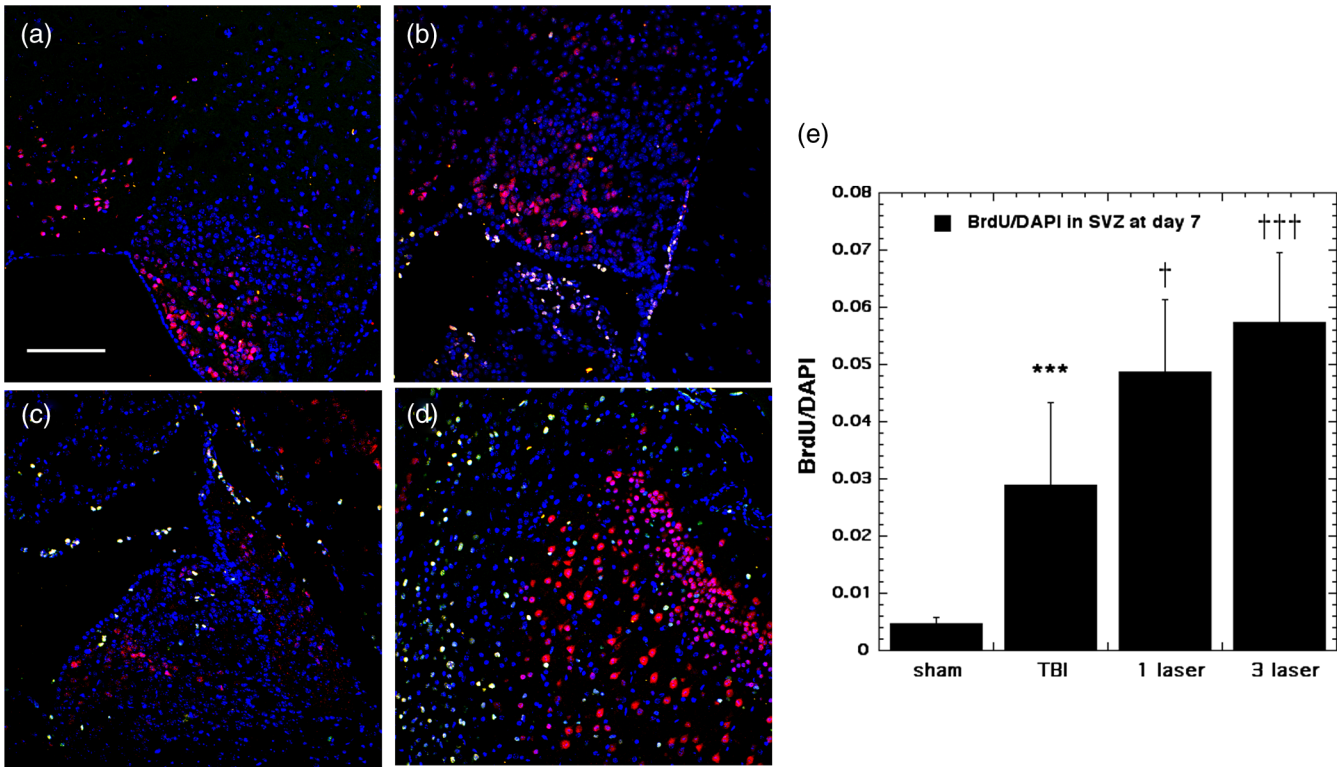


Fig. 6 BrdU-NeuN double-staining images and analyses at the neurogenic subventricular zone (SVZ) at the 7 days point; (a) sham, (b) CCI-TBI, (c) 1× tLLLT, (d) 3× tLLLT, (e) mean BrdU/DAPI ratios ± SD ($n = 5$); normalization of the readings was done BrdU versus DAPI (labeling the nuclei). Scale bar 100 μm . *** $p < 0.001$ versus sham; †, ††† $P < 0.05, 0.001$ versus TBI.

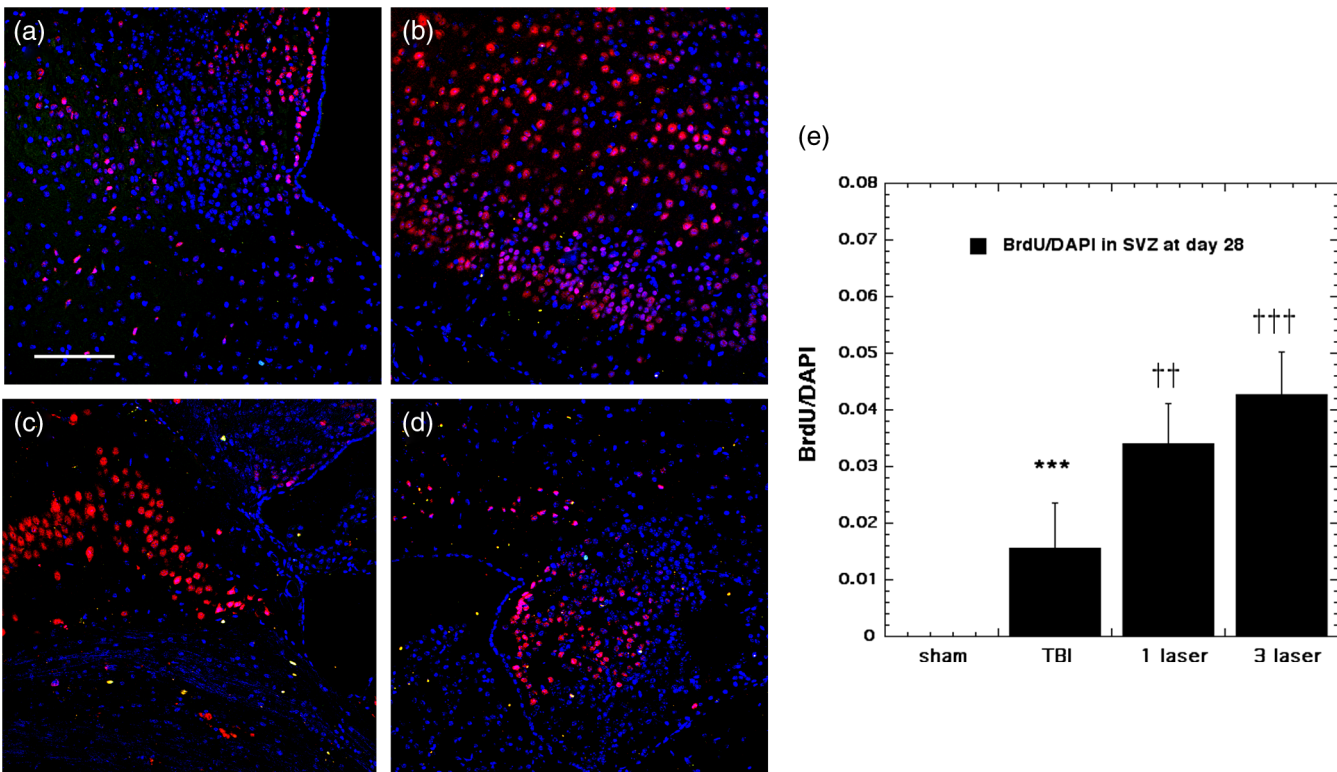


Fig. 7 BrdU-NeuN double-staining images and analyses at the neurogenic SVZ at the 28 days point; (a) sham, (b) CCI-TBI, (c) 1× tLLLT, (d) 3× tLLLT, (e) mean BrdU/DAPI ratios ± SD ($n = 5$); normalization of the readings was done BrdU versus DAPI (labeling the nuclei). Scale bar 100 μm . *** $p < 0.001$ versus sham; ††, ††† $P < 0.01, 0.001$ versus TBI.

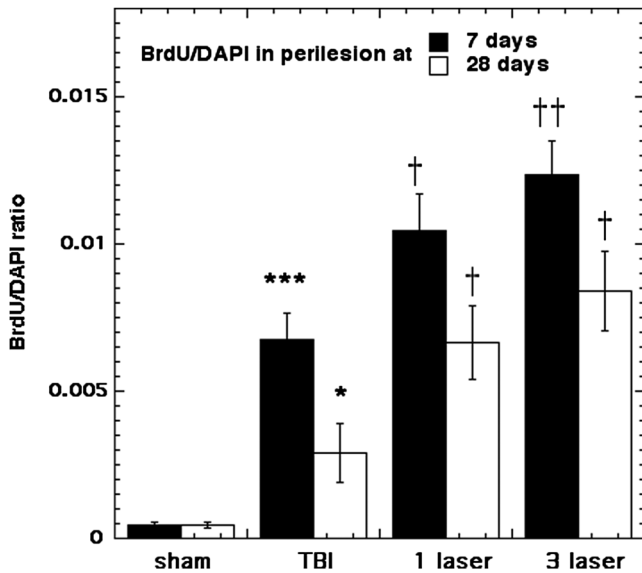


Fig. 8 BrdU incorporating cells at the lesion site at the 7- and 28-days points. Mean BrdU/DAPI ratios \pm SD ($n = 5$). *, *** $P < 0.05$, 0.001 versus sham; †, †† $P < 0.05$, 0.01 versus TBI.

($p < 0.0001$) in latency ($44 - 36 \pm 4$ s) in TBI mice compared to normal ($11 - 10 \pm 1$ s) and sham ($18 - 14 \pm 2$ s) groups. The 1 \times tLLLT group had significant improvements ($p < 0.0001$) in latency ($34 - 26 \pm 5$ s) versus TBI. The 3 \times tLLLT latency was

significantly ($p < 0.05$) better than the 1 \times tLLLT latency at the second and fourth repetitions. The rate of learning (gradient between the five successive repetitions) did not appear to be different between the TBI and the 1 \times tLLLT and 3 \times tLLLT groups.

For the latency with the probe test, TBI mice had a large ($p < 0.001$) increase (35 ± 4 s) compared to normal (8 ± 1 s) and sham-TBI mice (15 ± 3 s). Mice treated with 1 \times tLLLT had a significant ($p < 0.01$) improvement (26 ± 2 s), while mice that received 3 \times tLLLT had an even bigger ($p < 0.001$ versus TBI and $p < 0.05$ versus 1 \times tLLLT) improvement (22 ± 2 s), Fig. 2(c).

3.3 Caspase-3 Staining in Lesion Site

Caspase-3 expression in the injured region at day 4 of the TBI induction is shown in Fig. 3. The TBI sustaining cohort is expressing significant amounts of the protein ($p < 0.001$ versus sham) at the lesion site, whereas laser treatments are showing a significant declining trend of its expression; 1 \times tLLLT per day is $p < 0.05$ versus TBI and 3 \times tLLLT per day is $p < 0.01$ versus TBI. These findings imply that tLLLT can have a rapid cytoprotective effect by reducing apoptosis in the damaged lesion area. Moreover, although tLLLT suppressed the effector caspase 3, at the end of the chain of caspases, which are the main propagators of apoptosis at cellular level, it cannot be concluded at what stage of the cascade the LLLT had its primary effect.

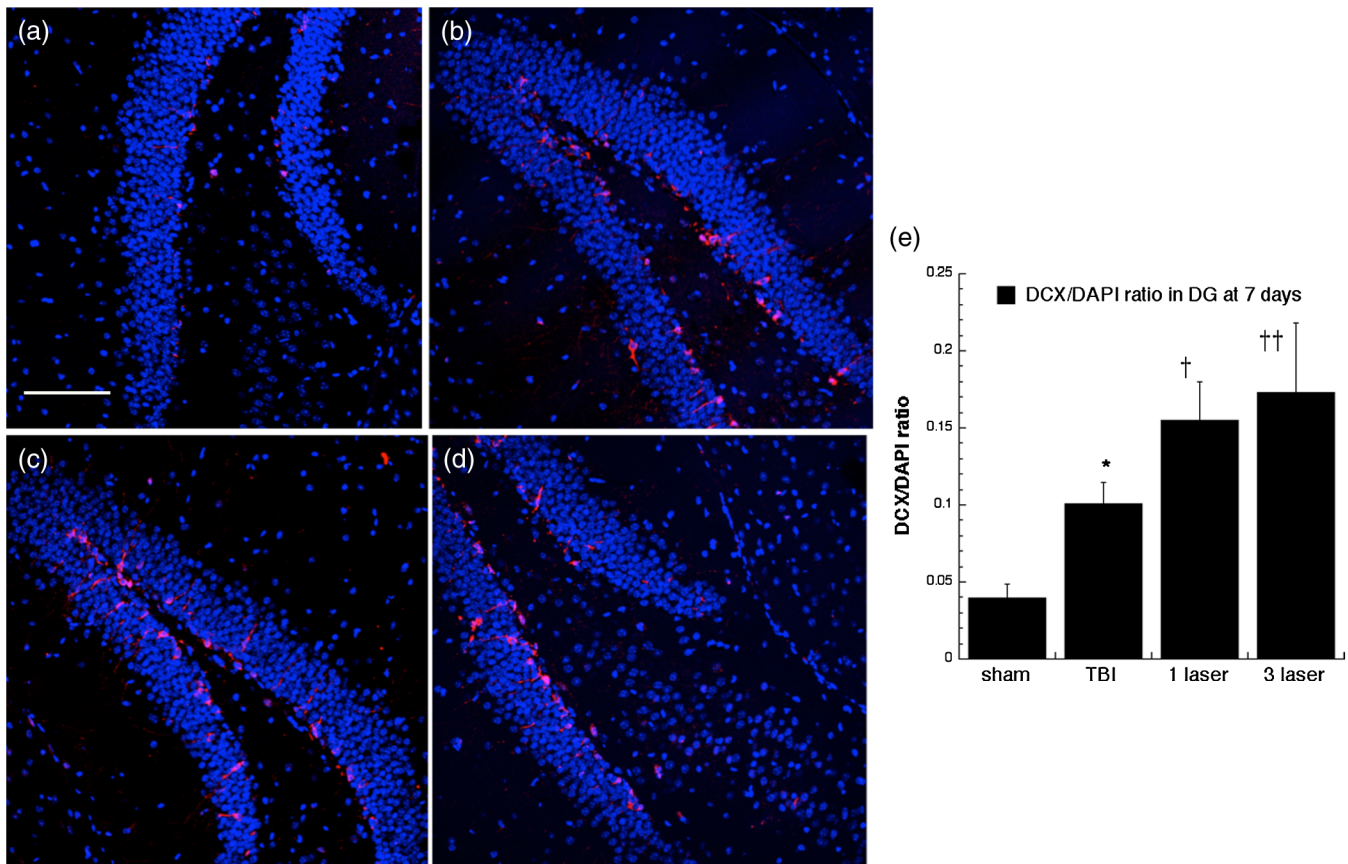


Fig. 9 Microtubule-associated neuronal migration protein (DCX) expression images and analyses at the neurogenic hippocampal DG at the 7 days point; (a) sham, (b) CCI-TBI, (c) 1xtLLLT, (d) 3xtLLLT, (e) mean DCX/DAPI ratios \pm SD ($n = 5$); normalization of the readings was done DCX versus DAPI (labeling the nuclei). Scale bar 100 μ m. * $p < 0.05$ versus sham; †, †† $P < 0.05$, 0.01 versus TBI.

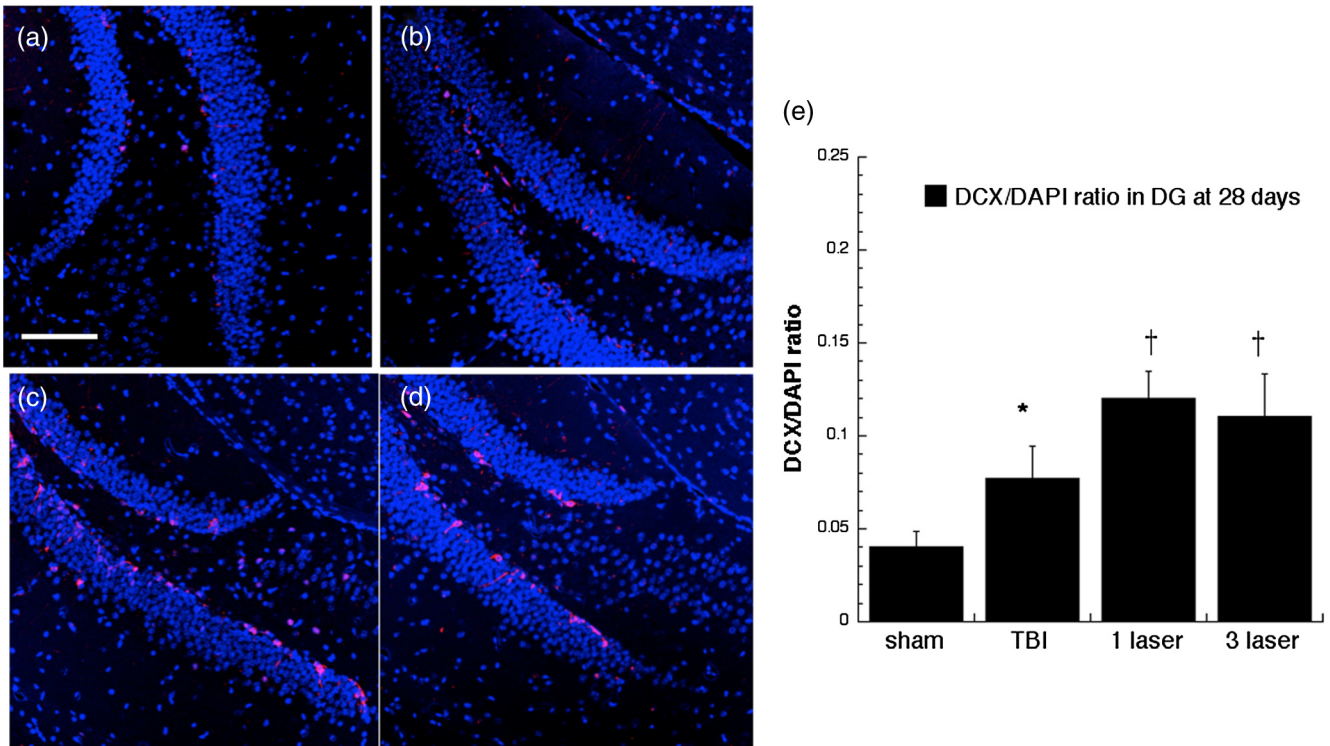


Fig. 10 Microtubule-associated neuronal migration protein (DCX) expression images and analyses at the neurogenic hippocampal DG at the 28 days point; (a) sham, (b) CCI-TBI, (c) 1× tLLLT, (d) 3× tLLLT, (e) mean DCX/DAPI ratios ± SD ($n = 5$); normalization of the readings was done DCX versus DAPI (labeling the nuclei). Scale bar 100 μm . * $p < 0.05$ versus sham; † $P < 0.05$ versus TBI.

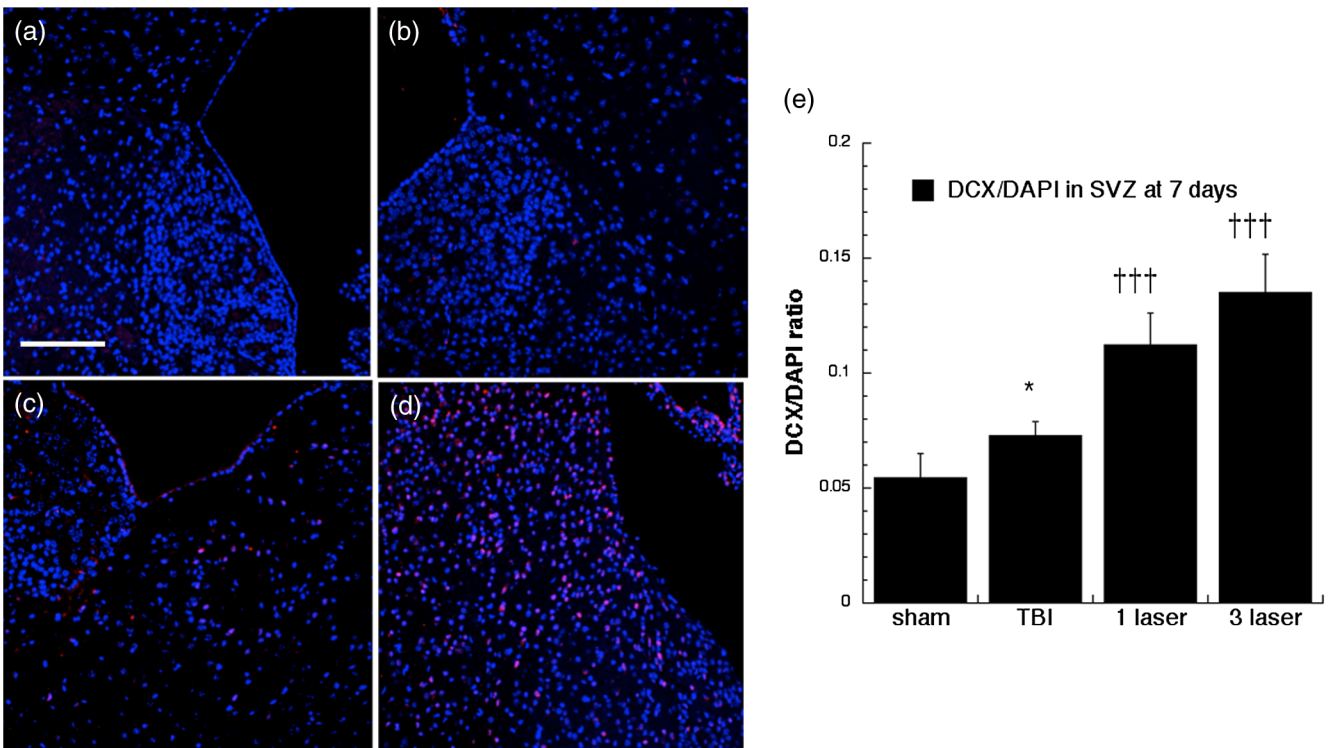


Fig. 11 Microtubule-associated neuronal migration protein (DCX) expression images and analyses at the neurogenic SVZ at the 7 days point; (a) sham, (b) CCI-TBI, (c) 1× tLLLT, (d) 3× tLLLT, (e) mean DCX/DAPI ratios ± SD ($n = 5$); normalization of the readings was done DCX versus DAPI (labeling the nuclei). Scale bar 100 μm . * $p < 0.05$ versus sham; ††† $P < 0.001$ versus TBI.

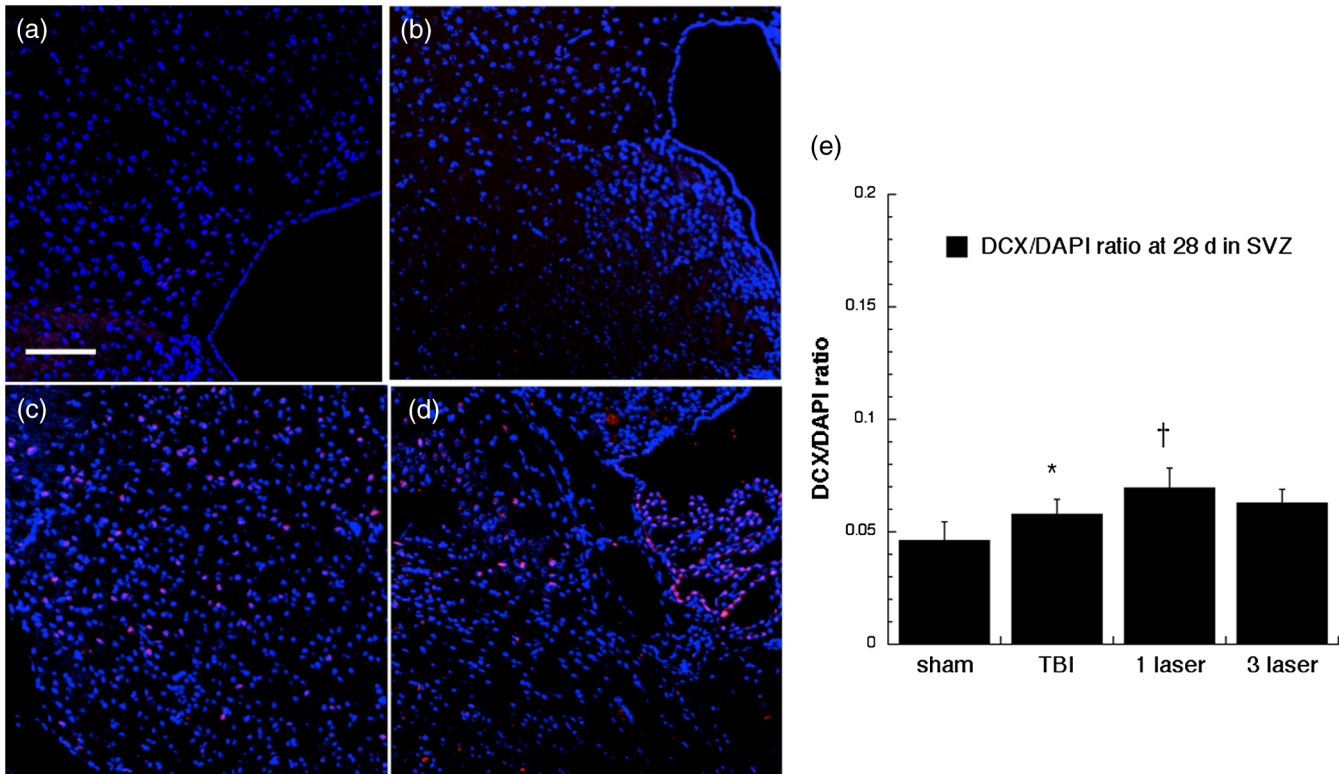


Fig. 12 Microtubule-associated neuronal migration protein (DCX) expression images and analyses at the neurogenic SVZ at the 28 days point; (a) sham, (b) CCI-TBI, (c) 1× tLLLT, (d) 3× tLLLT, (e) mean DCX/DAPI ratios ± SD ($n = 5$); normalization of the readings was done DCX versus DAPI (labeling the nuclei). Scale bar 100 μm . * $p < 0.05$ versus sham; † $P < 0.05$ versus TBI.

3.4 BrdU-NeuN Expression

To show neurogenesis, we used the double labeling technique with co-staining for BrdU and NeuN where BrdU labels newly generated cells whose DNA has replicated, and NeuN is a

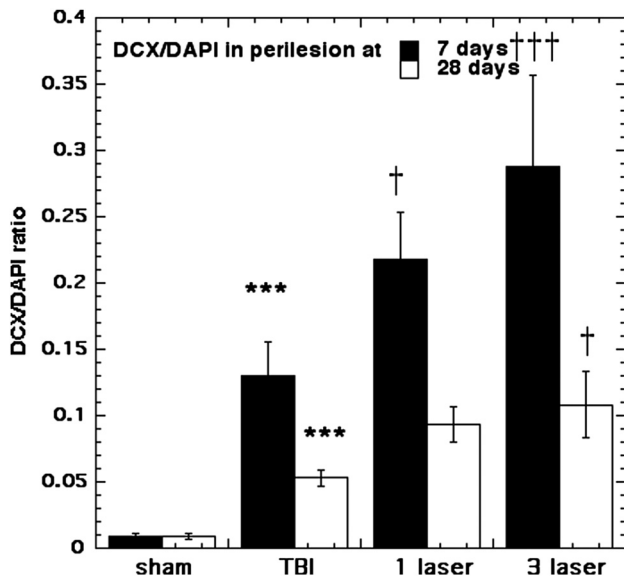


Fig. 13 Microtubule-associated neuronal migration protein (DCX) expression at the lesion site. Mean DCX/DAPI ratios ± SD ($n = 5$); normalization of the readings was done as DCX versus DAPI (labeling the nuclei). *** $p < 0.001$ versus sham; †, ††† $P < 0.05, 0.001$ versus TBI.

specific label for postmitotic mature neurons just before synaptic integration.²⁵ We concentrated on two areas in the mouse brain; the subgranular layer of the hippocampal DG and the sub-ventricular zone (SVZ) of the lateral ventricle.^{26,27} Both these areas of the rodent brain are well known to give rise to neuro-progenitor cells both after TBI²⁸ and after other interventions that have been tested for possible neuroprotective and neuro-regenerative effects.^{29,30} The two time points of analysis were 7 days and 28 days after the TBI induction. It should be noted that virtually all BrdU positive cells observed were pink, indicating triple staining (BrdU + NeuN) and DAPI and blue-green BrdU + DAPI alone, which would be expected from newly formed glial cells. The normalization of the BrdU-NeuN double stained cells was done by counting the ratio of BrdU expression to DAPI staining (labeling cell nuclei). This was to correct for variation in the numbers of cells visible in different sections.

Our results indicated that some neurogenesis was caused by TBI alone in the DG both at 7 days (Fig. 4) and at 28 days (Fig. 5). However, significant ($p < 0.05$) further increases were generated by 1× tLLLT ($p < 0.01$ versus TBI), 3× tLLLT ($p < 0.001$ versus TBI), and ($p < 0.001$ versus sham) at 7 days. Note in Fig. 4(d), (3× tLLLT) the double stained cells are clearly visible lining the subgranular layer. At 28 days post-TBI, the laser induction of neurogenesis in the DG appears to be more modest.

There was a large increase in BrdU-NeuN cells in the SVZ at day 7 in TBI mice ($p < 0.001$ versus sham), Fig. 6. The values were further increased by 1× tLLLT ($p < 0.05$ versus TBI) and by 3× tLLLT ($p < 0.001$ versus TBI). The increase in BrdU-NeuN in the SVZ at day 28 post-TBI (Fig. 7) was

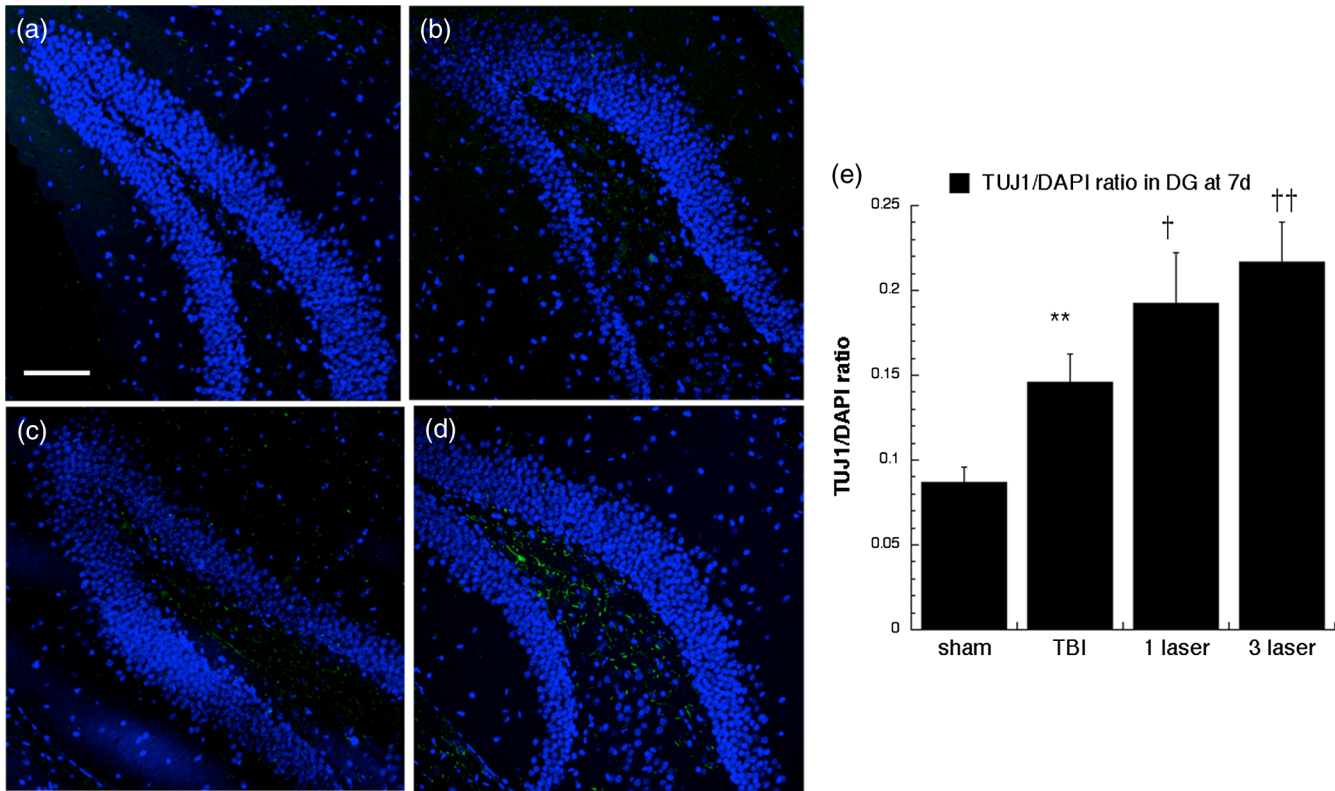


Fig. 14 Neuron-specific class III β -tubulin (TUJ-1) expression in differentiating neural progenitor cells of the DG at 7 days point. Images are for (a) sham, (b) CCI-TBI, (c) 1 \times tLLLT, (d) 3 \times tLLLT brain slices, (e) mean TUJ-1/DAPI ratios \pm SD ($n = 5$); normalization of the readings was done TUJ-1 versus DAPI (labeling the nuclei). Scale bar 100 μ m. ** $p < 0.01$ versus sham; †, †† $P < 0.05, 0.01$ versus TBI.

much lower (0.03 ± 0.009), but the value was more than doubled (0.068 ± 0.009 , $p < 0.05$) by 1 \times tLLLT and further increased by 3 \times tLLLT (0.078 ± 0.009 , $p < 0.01$).

BrdU/DAPI expression at the lesion site at the 7- and 28-days points is shown in Fig. 8, indicating that TBI induction has triggered a remarkable cell proliferation process at the lesion, especially at the 7-day point ($p < 0.001$ versus sham), and laser application has been shown to amplify this process; 1 \times tLLLT $p < 0.05$ versus TBI and 3 \times tLLLT $p < 0.01$ versus TBI. The cell proliferation process appears to be effective during the 28-day point as well albeit with more modest expressions. In our previous study, we had only looked at BrdU incorporation at the 28-day timepoint.¹²

3.5 Double-Cortin Expression

Double-cortin (DCX) is a microtubule-associated protein expressed by neuronal precursor cells and immature neurons in embryonic and adult cortical structures. Neuronal precursor cells begin to express DCX while actively dividing, and their neuronal daughter cells continue to express DCX for 2–3 weeks as the cells mature into neurons.³¹

Figures 9 through 12 show our results for DCX expression at the two points of time lines, days 7 and 28, at the neurogenic DG and SVZ regions. The microtubule-associated neuronal migration protein DCX expression images and analyses at the neurogenic hippocampal DG at the 7 day point are given in Fig. 9. There was only a moderate increase in DCX staining caused by TBI alone in the DG at 7 days ($p < 0.05$ versus sham). However, 1 \times tLLLT and 3 \times tLLLT produced significant ($p < 0.05$ and

$p < 0.01$) increases in DCX expression compared to TBI alone at 7 days (but not at 28 days, Fig. 10) both in the DG and also in the SVZ (Fig. 11). Interestingly, DCX levels in the SVZ were significantly increased after 1 \times and 3 \times tLLLT application ($p < 0.001$) at the 7-day time-point in comparison with the DCX levels, expressed by TBI alone mice, Fig. 11. The effect diminished with only very modest expression at the 28-day time point, Fig. 12. DCX expression at the lesion site, Fig. 13, after the TBI induction was significantly elevated ($p < 0.001$ versus sham) during both the 7- and 28-day time points with 1 \times tLLLT and 3 \times tLLLT levels being especially increased at the 7-day period versus TBI-induced cohorts, with 7 days 3 \times tLLLT $p < 0.001$ versus TBI. Overall, this remarkable increase in the level of DCX expressing cells at the lesion of the TBI sustained cohorts (in both timelines $p < 0.001$ versus sham) with especially pronounced elevations in the 3 \times tLLLT applied cohort ($p < 0.001$ versus TBI) may be indicative of the elevated numbers of migrating neuroprogenitors and the laser protective effects on the neuroprogenitors in migration.

3.6 TUJ-1 Expression

TUJ-1 recognizes a neuron-specific class III beta-tubulin whose expression has been found to be an early molecular event in neuronal differentiation and is exhibited by a wide range of neuronal precursors.³² Our results for TUJ-1 staining (used to distinguish the immature postmitotic neurons, just before synaptic integration) are given in Figs. 14, 15, 16, and 17. One can see that TBI alone only produced an increase in the DG at 7 days. However, 1 \times tLLLT and 3 \times tLLLT produced significant ($p < 0.05$ and

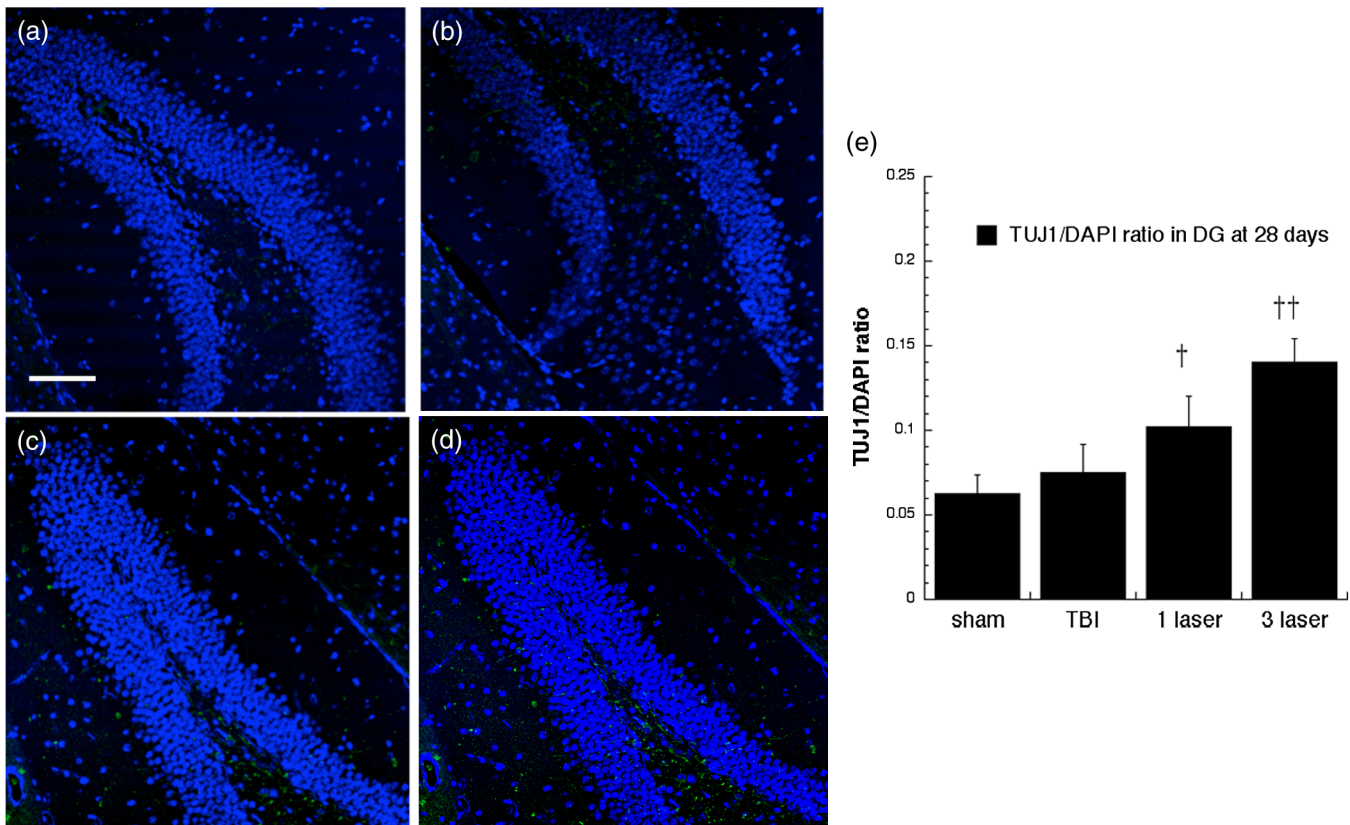


Fig. 15 Neuron-specific class III β -tubulin (TUJ-1) expression in differentiating neural progenitor cells of DG at 28 days point. Images are from (a) sham, (b) CCI-TBI, (c) 1 \times tLLLT, (d) 3 \times tLLLT brain slices, (e) mean TUJ-1/DAPI ratios \pm SD ($n = 5$); normalization of the readings was done TUJ-1 versus DAPI (labeling the nuclei). Scale bar 100 μ m. †, †† $P < 0.05$, 0.01 versus (TBI).

$p < 0.01$, respectively) increases in TUJ-1 compared to TBI alone at both time points (days 7 and 28) in both neurogenic areas of the brain, SVZ, and DG. One can see that the postmitotic TUJ-1-positive cells, generated throughout the period of cortical neurogenesis, were abundant in the 1 \times and 3 \times laser treated cohorts. 3 \times tLLLT appeared to prolong the lifetime of the adult neuroprogenitors as indicated by the significant levels of TUJ-1 expression in the neurogenic hippocampal DG even at day 28 after TBI induction ($p < 0.01$ versus TBI). In the other neurogenic hot spot, the SVZ, 3 \times LLLT was also effective with $p < 0.01$ versus TBI at the day 7 point and $p < 0.05$ versus TBI at the 28-day point, where at day 28, only the 3 \times tLLLT exposed cohorts show elevated levels of TUJ-1 expressing neuroprogenitors.

4 Discussion

We had previously reported¹⁰ that tLLLT using the parameters described in the present study (36 J/cm² of 810-nm laser delivered at 50 mW/cm² and 12 min) delivered to mice who received a severe CCI-TBI 4 h previously had beneficial effects in improving the NSS and reducing the size of the brain lesion as measured by histology. In a subsequent study,¹² we showed that a lower dose of tLLLT (18 J/cm² delivered at 25 mW/cm² and in 12 min) was more effective with regard to improving the NSS if repeated once a day for 3 days, than if given a single time (4-h post-TBI) or if given once a day for 14 days. We obtained some evidence that cells around the lesion incorporated BrdU after tLLLT, suggesting that they were either proliferating

neuronal cells or activated glial cells.¹² If these cells were proliferating neuronal cells, they could be expected to have originated in one of the two neurogenic areas of the rodent brain that have been identified to contain so-called NSCs or neuroprogenitor cells, the DG, and SVZ.

In the present study, we used the accepted method of labeling proliferating neural cells, which is double staining with BrdU and the mature neuronal marker NeuN. We also looked into the expression of other well-known neural cell markers such as DCX and TUJ-1.

As previously found,¹² the 1 \times tLLLT and to a greater extent the 3 \times tLLLT treated mice had improved neurological performance as measured by improved motor function performance in the WGMT. We used the MWM as a more advanced way to measure cognitive function in terms of spatial learning and memory. The improvement in latency produced by tLLLT (3 \times tLLLT was even better than 1 \times tLLLT) in the visible platform, the hidden platform and the probe test suggested that spatial memory and cognitive perception were improved by tLLLT, while the absence of a significantly steeper gradient in the five successive hidden platform tests suggested that learning was not specifically improved by tLLLT. The only other report of improvement in MWM performance in mice by application of tLLLT was by Khuman et al.³³ who delivered an 800-nm laser either transcranially or through an open craniotomy to C57BL/6 mice with CCI-TBI. There was a significant decrease in latency to the hidden platform and improvement in probe trial performance compared to untreated controls but only with

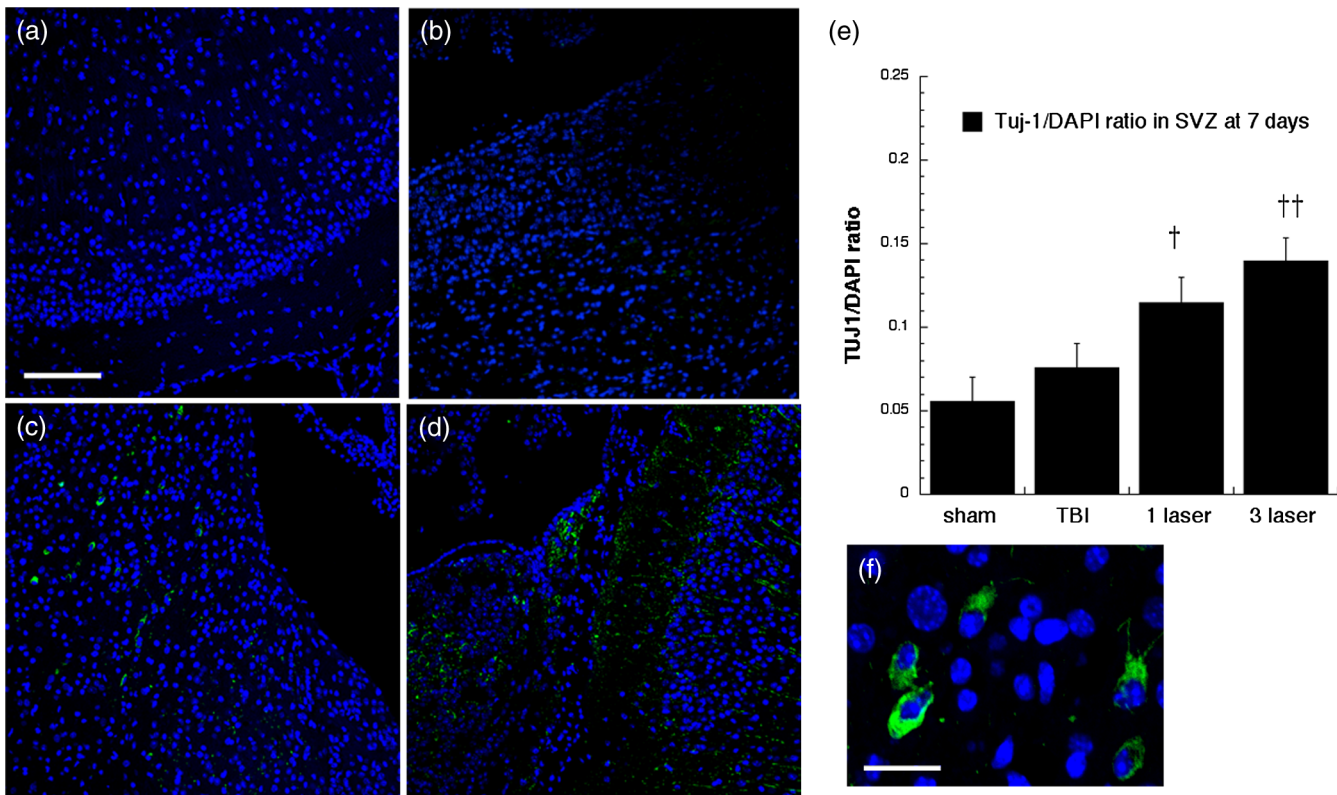


Fig. 16 Neuron-specific class III β -tubulin (TUJ-1) expression in differentiating neural progenitor cells of SVZ at 7 days point. Images are for (a) sham, (b) CCI-TBI, (c) 1 \times tLLLT, (d) 3 \times tLLLT, (e) mean TUJ-1/DAPI ratios \pm SD ($n = 5$), and (f) close look up brain slices; normalization of the readings was done TUJ-1 versus DAPI (labeling the nuclei). Scale bar 100 μ m, except in (f) where it is 25 μ m. †, †† $P < 0.05$, 0.01 versus TBI.

certain parameters. Histological investigations proposed a reduction in inflammation (activated microglia) to be (partly) responsible for the benefit.

A study from Oron's lab showed the effectiveness of tLLLT in mice with TBI manifested by improvements in NSS and corresponding reductions in lesion size in Sabra mice with a single exposure to 808-nm LLLT.¹⁴ A follow-up study showed that the pulse structure and the time between injury and irradiation was important in defining how much benefit the LLLT provided to the mice.¹⁵

Quirk et al.³⁴ used the TruScan nose poke test to follow the response of Sprague-Dawley rats with CCI-TBI to tLLLT (670 nm, 5 min, 50 mW/cm², 15 J/cm²) per day for 10 days. They found significant reductions in task entries, repeat entries, and task errors that coincided with a decrease in Bax and an increase in Bcl2.

De Taboada et al. showed³⁵ remarkable improvements in MWM performance by delivering tLLLT in a transgenic mouse model that expresses amyloid-beta protein precursor and which develops pathology similar to Alzheimer's disease. tLLLT was administered three times/week at various doses, starting at 3 months of age, and mice were examined for amyloid load, inflammatory markers, amyloid-beta (A-beta) levels, and changes in cognitive function. The numbers of A-beta plaques and amyloid load were significantly reduced in the brain with administration of tLLLT in a dose-dependent fashion. All doses improved the cognitive defects seen with advanced amyloid deposition and reduced the expression of inflammatory

markers. In addition, tLLLT showed an increase in ATP levels, mitochondrial function, and c-fos suggesting an overall improvement in neurological function.

Many of these improvements in brain function that have been observed when tLLLT was used in mice with various neurological injuries and diseases, may possibly be explained by the process of neurogenesis. One hypothesis for LLLT stimulation of neurogenesis is that tLLLT stimulates the mitochondria of neural stem cells and neuroprogenitor cells, and thus induces them to mobilize out of their hypoxic niche and assume a differentiated and proliferating phenotype. Our findings that neurogenesis in the DG and SVZ was more pronounced at 7 days post-TBI than at 28 days are intriguing. The fact that markers of migrating neuroprogenitor cells (DCX and TUJ-1) were also upregulated in the DG and SVZ along with BrdU incorporation implies that these newly formed neurons have the capacity to at least move from the exact site where they were created. In the present study, to monitor the neurogenesis and migration, we used DCX, NeuN, and TUJ-1. The DCX is nearly exclusively expressed in developing neurons and the downregulation of DCX begins (2 weeks after generation) and takes place while, in tandem, the same cells begin expressing the NeuN (a marker for mature neurons³⁶). The neuron-specific class III beta-tubulin (TUJ-1), the expression of which represents an early molecular event in neuronal differentiation, is exhibited by a wide range of neuronal precursors.³² In an earlier study, Menezes³⁷ has shown that double labeled BrdU- TUJ-1 positive cells were postmitotic and generated throughout the period of cortical neurogenesis and

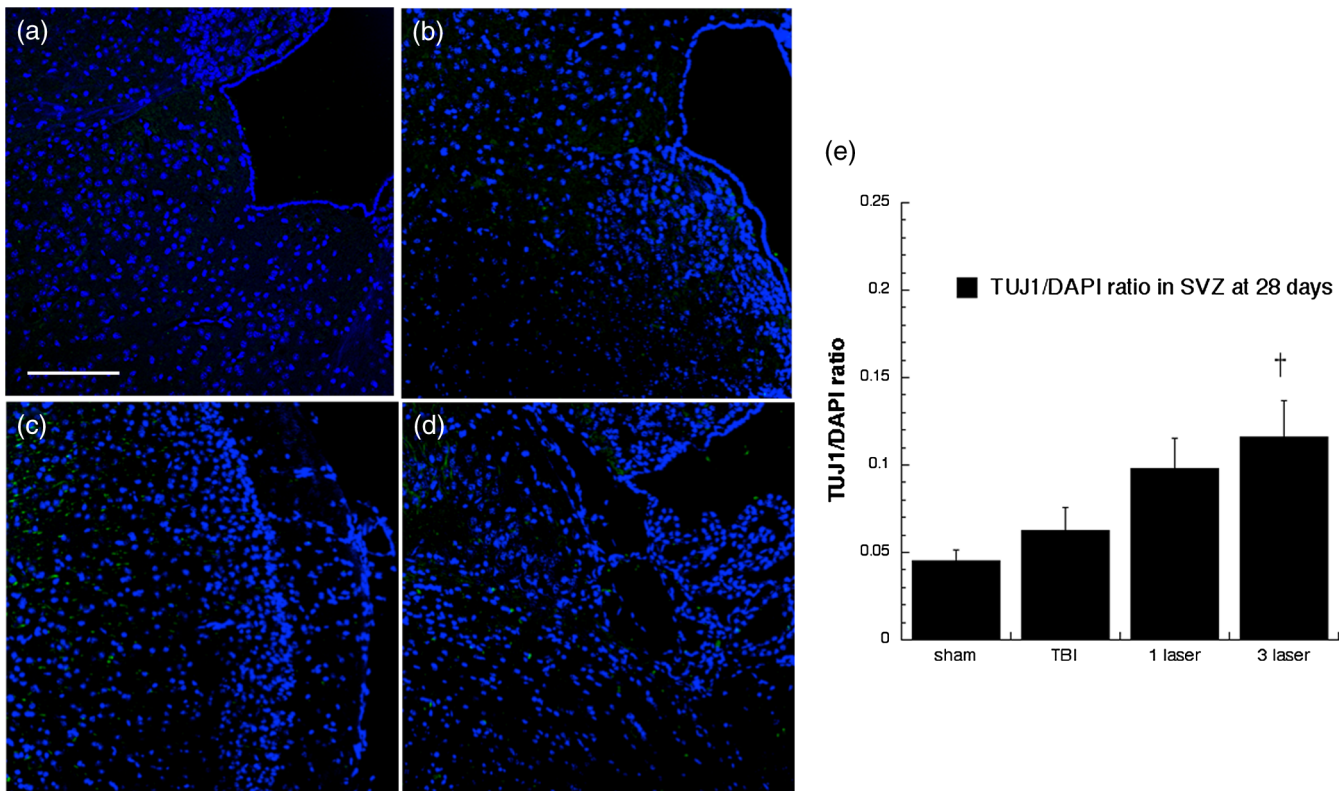


Fig. 17 Neuron-specific class III β -tubulin (TUJ-1) expression in differentiating neural progenitor cells of subventricular zone (SVZ) at 28 days point. Images are for (a) sham, (b) CCI-TBI, (c) 1 \times tLLLT, (d) 3 \times tLLLT, (e) mean TUJ-1/DAPI ratios \pm SD ($n = 5$); normalization of the readings was done TUJ-1 versus DAPI (labeling the nuclei). Scale bar 100 μ m. † $P < 0.05$ versus TBI.

that TUJ-1 immunoreactivity actually distinguishes two neuronal populations: those that remain for an indefinite period of time in the proliferative zones and those that leave the proliferative zones soon after being generated, and their distribution suggests that they migrate independent of radial glial fibers, which is corroborating the findings of our study.

Although we did not measure lesion size in the present study, in two previous studies, we were able to show that the lesion size after CCI TBI was smaller in tLLLT treated mice than TBI control mice, especially at later time points (2–4 weeks post-TBI). The possible reasons for this may be twofold. First is the ability of tLLLT to protect tissue at risk of dying by upregulating cytoprotective pathways such as anti-apoptotic proteins.³⁸ The effect of tLLLT on increasing the mitochondrial membrane potential^{39,40} may stabilize the mitochondria and/or prevent the opening of the mitochondrial permeability transition pore that is a well-known initiator of apoptosis.⁴¹ Caspase-3 is known to be activated via both extrinsic (cell ligands) and intrinsic (mitochondrial assembly of pro-apoptotic factors) pathways in apoptotic cells.^{42,43} Kaneko et al. study⁴⁴ revealed that caspase-3 mRNA expression was slightly elevated at 8 h post-TBI induction but was not significantly upregulated up until the 48th hour and caspase-3 immunoreactive cells were not found until 48 h after the induction. In tandem with these findings and our results, the emerging picture is clearly suggesting that immediately after the TBI induction, the injured brain attempts to repair itself (via neuronal cell proliferation). However, this endogenous regenerative mechanism may not be sufficient to abrogate the secondary apoptotic cell death. But when we introduce the tLLLT,

the study cohorts are revealing that it amplifies the cell proliferation and reduces apoptosis. This ability of tLLLT to protect tissue has long been supposed to be responsible for the lesser areas/volumes of damage in such animal models as ischemic cardiac damage⁴⁵ and thrombotic stroke.⁴⁶ However, our present data suggest that there may be another mechanism of action operating after tLLLT that we can describe as “tLLLT can induce the brain to repair itself.” In fact, it could be the case that part of the reason why the tLLLT treated TBI mice had smaller lesions than the TBI control mice was that the light had caused neuroprogenitor cells to proliferate in the DG and SVZ and then to migrate to the site of injury to repair the damage. This is partly corroborated by our previous finding¹² that tLLLT increased BrdU incorporation in the region of the injured cortex at 28 days post-TBI. Oron et al. found⁴⁶ similar results in a rat model of stroke where neuroprogenitor cells were found in the SVZ at 28 days poststroke (LLLT was delivered 24 h-poststroke).

5 Conclusion

We have shown, for the first time, that tLLLT can stimulate neurogenesis in both the hippocampal DG and the SVZ in mice with TBI. Moreover, the treatment has been shown to improve spatial memory and learning. The likelihood that LLLT can induce the brain to repair itself after injury suggests that laser therapy may have much wider applications than that previously considered. Many diseases of the brain that are traumatic, degenerative, and psychiatric could be benefited if neurogenesis can be induced by an inexpensive, low-risk procedure without known side-effects.

Moreover, tLLLT appears to be a viable and efficient stimulus for enhancing endogenous neurogenesis and to exert a survivability enhancing effect on the neuroprogenitor cells, thus increasing their chance to get functionally integrated into the pre-existing neuronal circuitry. In our study, both cognitive performance and neuromotor assessment test studies corroborated the immunohistochemical findings. However, more complementary *in vivo* imaging studies can *in situ* reveal the effects of tLLLT on the surge of neuroprogenitors into the injured area and the migratory effects of NSCs in brain functioning, homeostasis, and the effective treatment of various neurologic diseases.

Acknowledgments

This work was supported by US NIH Grant No. R01AI050875, by Air Force Office of Scientific Research Grant No. FA9550-13-1-0068, by US Army Medical Research Acquisition Activity Grant No. W81XWH-09-1-0514 and by US Army Medical Research and Materiel Command Grant No. W81XWH-13-2-0067.

References

- B. Roozenbeek et al., "Predicting 14-day mortality after severe traumatic brain injury: application of the IMPACT models in the Brain Trauma Foundation TBI-trac(R) New York State database," *J. Neurotrauma* **29**(7), 1306–1312 (2012).
- R. C. Opreanu, D. Kuhn, and M. D. Basson, "Influence of alcohol on mortality in traumatic brain injury," *J. Am. Coll. Surg.* **210**(6), 997–1007 (2010).
- J. Dubourg and M. Messerer, "Sports-related chronic repetitive head trauma as a cause of pituitary dysfunction," *Neurosurg. Focus* **31**(5), E2 (2011).
- K. S. Meyer et al., "Combat-related traumatic brain injury and its implications to military healthcare," *Psychiatr. Clin. North Am.* **33**(4), 783–96 (2010).
- D. J. Loane and A. I. Faden, "Neuroprotection for traumatic brain injury: translational challenges and emerging therapeutic strategies," *Trends Pharmacol. Sci.* **31**(12), 596–604 (2010).
- H. Chung et al., "The nuts and bolts of low-level laser (light) therapy," *Ann. Biomed. Eng.* **40**(2), 516–533 (2012).
- M. A. Naeser and M. R. Hamblin, "Potential for transcranial laser or LED therapy to treat stroke, traumatic brain injury, and neurodegenerative disease," *Photomed. Laser Surg.* **29**(7), 443–446 (2011).
- F. Schiffer et al., "Psychological benefits 2 and 4 weeks after a single treatment with near infrared light to the forehead: a pilot study of 10 patients with major depression and anxiety," *Behav. Brain Funct.* **5**, 46 (2009).
- Y. Y. Huang et al., "Biphasic dose response in low level light therapy," *Dose Response* **7**(4), 358–383 (2009).
- T. Ando et al., "Comparison of therapeutic effects between pulsed and continuous wave 810-nm wavelength laser irradiation for traumatic brain injury in mice," *PLoS ONE* **6**(10), e26212 (2011).
- Q. Wu et al., "Low level laser therapy for closed-head traumatic brain injury in mice: effect of different wavelengths," *Lasers Surg. Med.* **44**(3), 218–226 (2012).
- W. Xuan et al., "Transcranial low-level laser therapy improves neurological performance in traumatic brain injury in mice: effect of treatment repetition regimen," *PLoS ONE* **8**(1), e53454 (2013).
- J. Khuman et al., "Low-level laser light therapy improves cognitive deficits and inhibits microglial activation after controlled cortical impact in mice," *J. Neurotrauma* **29**, 408–417 (2012).
- A. Oron et al., "Low-level laser therapy applied transcranially to mice following traumatic brain injury significantly reduces long-term neurological deficits," *J. Neurotrauma* **24**(4), 651–656 (2007).
- U. Oron, "Near infrared transcranial laser therapy applied at various modes to mice following traumatic brain injury significantly reduces long-term neurological deficits," *J. Neurotrauma* **29**(2), 401–407 (2011).
- L. Bonfanti and P. Peretto, "Adult neurogenesis in mammals: a theme with many variations," *Eur. J. Neurosci.* **34**(6), 930–950 (2011).
- C. Zhang et al., "Role of transcription factors in neurogenesis after cerebral ischemia," *Rev. Neurosci.* **22**(4), 457–465 (2011).
- R. M. Richardson, D. Sun, and M. R. Bullock, "Neurogenesis after traumatic brain injury," *Neurosurg. Clin. North Am.* **18**(1), 169–181 (2007).
- Y. Mu and F. H. Gage, "Adult hippocampal neurogenesis and its role in Alzheimer's disease," *Mol. Neurodegener.* **6**, 85 (2011).
- N. D. Hanson, M. J. Owens, and C. B. Nemeroff, "Depression, antidepressants, and neurogenesis: a critical reappraisal," *Neuropsychopharmacology* **36**(13), 2589–2602 (2011).
- P. Beukelaers et al., "Cycling or not cycling: cell cycle regulatory molecules and adult neurogenesis," *Cell Mol. Life Sci.* **69**(9), 1493–1503 (2012).
- I. Masiulis, S. Yun, and A. J. Eisch, "The interesting interplay between interneurons and adult hippocampal neurogenesis," *Mol. Neurobiol.* **44**(3), 287–302 (2011).
- S. Bovetti et al., "From progenitors to integrated neurons: role of neurotransmitters in adult olfactory neurogenesis," *J. Chem. Neuroanat.* **42**(4), 304–316 (2011).
- K. Bromley-Brits, Y. Deng, and W. Song, "Morris water maze test for learning and memory deficits in Alzheimer's disease model mice," *J. Vis. Exp.* **53**(53), 2920 (2011).
- F. R. Sharp, J. Liu, and R. Bernabeu, "Neurogenesis following brain ischemia," *Brain Res. Dev. Brain Res.* **134**(1–2), 23–30 (2002).
- M. Brus, M. Keller, and F. Levy, "Temporal features of adult neurogenesis: differences and similarities across mammalian species," *Front. Neurosci.* **7**, 135 (2013).
- E. J. Kim et al., "Ascl1 (Mash1) defines cells with long-term neurogenic potential in subgranular and subventricular zones in adult mouse brain," *PLoS ONE* **6**(3), e18472 (2011).
- L. Zhang et al., "Survivin, a key component of the Wnt/beta-catenin signaling pathway, contributes to traumatic brain injury-induced adult neurogenesis in the mouse dentate gyrus," *Int. J. Mol. Med.* **32**(4), 867–875 (2013).
- S. Acosta et al., "NT-020, a natural therapeutic approach to optimize spatial memory performance and increase neural progenitor cell proliferation and decrease inflammation in the aged rat," *Rejuvenation Res.* **13**(5), 581–588 (2010).
- X. Xiao et al., "Neuroprotection and enhanced neurogenesis by tetramethylpyrazine in adult rat brain after focal ischemia," *Neurol. Res.* **32**(5), 547–555 (2010).
- O. von Bohlen Und Halbach, "Immunohistological markers for staging neurogenesis in adult hippocampus," *Cell Tissue Res.* **329**(3), 409–420 (2007).
- S. P. Memberg and A. K. Hall, "Dividing neuron precursors express neuron-specific tubulin," *J. Neurobiol.* **27**(1), 26–43 (1995).
- J. Khuman et al., "Low-level laser light therapy improves cognitive deficits and inhibits microglial activation after controlled cortical impact in mice," *J. Neurotrauma* **29**(2), 408–417 (2012).
- B. J. Quirk et al., "Near-infrared photobiomodulation in an animal model of traumatic brain injury: improvements at the behavioral and biochemical levels," *Photomed. Laser Surg.* **30**(9), 523–529 (2012).
- L. De Taboada et al., "Transcranial laser therapy attenuates amyloid-beta peptide neuropathology in amyloid-beta protein precursor transgenic mice," *J. Alzheimers Dis.* **23**(3), 521–535 (2011).
- S. Couillard-Despres et al., "Doublecortin expression levels in adult brain reflect neurogenesis," *Eur. J. Neurosci.* **21**(1), 1–14 (2005).
- J. R. Menezes and M. B. Luskin, "Expression of neuron-specific tubulin defines a novel population in the proliferative layers of the developing telencephalon," *J. Neurosci.* **14**(9), 5399–5416 (1994).
- J. Chu, S. Wu, and D. Xing, "Survivin mediates self-protection through ROS/cdc25c/CDK1 signaling pathway during tumor cell apoptosis induced by high fluence low-power laser irradiation," *Cancer Lett.* **297**(2), 207–219 (2010).
- Y. Y. Huang et al., "Low-level laser therapy (810 nm) protects primary cortical neurons against excitotoxicity *in vitro*," *J. Biophotonics* **7**(8), 656–664 (2013).
- Y. Y. Huang et al., "Low-level laser therapy (LLLT) reduces oxidative stress in primary cortical neurons *in vitro*," *J. Biophotonics* **6**(10), 829–838 (2013).
- S. Ghavami, "Autophagy and apoptosis dysfunction in neurodegenerative disorders," *Prog. Neurobiol.* **112**, 24–49 (2014).

42. G. S. Salvesen, "Caspases: opening the boxes and interpreting the arrows," *Cell Death Differ.* **9**(1), 3–5 (2002).
43. S. Ghavami et al., "Apoptosis and cancer: mutations within caspase genes," *J. Med. Genet.* **46**(8), 497–510 (2009).
44. Y. Kaneko et al., "Nestin overexpression precedes caspase-3 upregulation in rats exposed to controlled cortical impact traumatic brain injury," *Cell Med.* **4**(2), 55–63 (2012).
45. N. Ad and U. Oron, "Impact of low level laser irradiation on infarct size in the rat following myocardial infarction," *Int. J. Cardiol.* **80**(2–3), 109–116 (2001).
46. A. Oron et al., "Low-level laser therapy applied transcranially to rats after induction of stroke significantly reduces long-term neurological deficits," *Stroke* **37**(10), 2620–2624 (2006).

Weijun Xuan worked as a physician from 1983, an associate professor and director from 1996, and a professor from 2003 in the Department of Otolaryngology in Guangxi University of Chinese Medicine, China. During this time he also received an MM from Henan Medical University, and a PhD degree from Huazhong University of Science and Technology, China. He served as a visiting professor and research scientist at Massachusetts Eye and Ear Infirmary, and Massachusetts General Hospital, Harvard Medical School from 2008 to 2012.

Fatma Vatanserver is a neurologist by training with master's and PhD degrees, and postdoctoral training in polymer science/nanomaterials and nanotechnology. She is a principal investigator at the Wellman Center for Photomedicine, Massachusetts General Hospital, and Department of Dermatology at Harvard Medical School. Her research interests are focused on brain functioning, neurophotonics, near-infrared light effects in neurologic disorders, and traumatic brain injury. Her research has been supported by NIH, USAFOSR, and foundations.

Liyi Huang received her MD and PhD degrees from Guangxi Medical University, China, at which she engaged in the clinical work of infectious diseases as a physician, an associate professor, and a professor in succession from 1996. She was trained as a postdoctoral fellow and worked as a research fellow at Massachusetts General Hospital, Harvard Medical School from 2007 to 2012.

Michael R. Hamblin is a principal investigator at the Wellman Center for Photomedicine at Massachusetts General Hospital, an associate professor of dermatology at Harvard Medical School, and is affiliated faculty at Harvard-MIT Division of Health Science and Technology. He has published 258 peer-reviewed articles and four major textbooks on PDT and photomedicine. He chairs the SPIE Photonics West conference "Mechanisms for low-level light therapy" and was honored by election as a Fellow of SPIE.